Published in final edited form as:
J Org Chem. 2013 March 1; 78(5): 2083–2090. doi:10.1021/jo302266t.

Mechanistic Studies of Wacker-Type Amidocyclization of Alkenes Catalyzed by (IMes)Pd(TFA)$_2$(H$_2$O): Kinetic and Stereochemical Implications of Proton Transfer†

Xuan Ye, **Paul B. White**, and **Shannon S. Stahl**
Department of Chemistry, University of Wisconsin-Madison, 1101 University Avenue, Madison, Wisconsin 53706

Shannon S. Stahl: stahl@chem.wisc.edu

Abstract

The stereochemical course of the amidopalladation of alkenes has important implications for the development of enantioselective Pd-catalyzed "Wacker-type" oxidative amination of alkenes. We have recently shown that the addition of base (Na_2CO_3) can alter the stereochemical course of amidopalladation in the (IMes)Pd(TFA)$_2$(H$_2$O)-catalyzed aerobic oxidative amidation of alkene. In this study, the mechanism of (IMes)Pd(TFA)$_2$(H$_2$O)-catalyzed oxidative heterocyclization of (*Z*)-4-hexenyltosylamide was investigated in the presence and absence of exogenous base Na_2CO_3. The results reveal two parallel pathways in the absence of base: a *cis*-amidopalladation pathway with turnover-limiting deprotonation of the sulfonamide nucleophile, and a *trans*-amidopalladation pathway with turnover-limiting nucleophilic attack of sulfonamide on the coordinated alkene. The addition of base (Na_2CO_3) lowers the energy barrier associated with the proton transfer, leading to an overall faster turnover rate and exclusive *cis*-amidopalladation of alkene.

Introduction

Palladium-catalyzed "Wacker-type" oxidative heterocyclizations provide efficient access to various classes of nitrogen-containing heterocycles.[2] In recent years, we[3] and others[4] have developed a number of aerobic oxidative cyclization methods with amide-type nucleophiles, including sulfonamides, sulfinamides, and carbamates, for syntheses of pyrrolidines and related heterocycles. In order to facilitate the development of enantioselective applications of these reactions, considerable effort has been directed toward understanding and controlling the stereochemical course of the amidopalladation step.[2i] Both *cis*-[5] and *trans*-amidopalladation[6] steps (Scheme 1) have been established in catalytic reactions, and various experimental approaches have been developed to probe these two pathways.[7–9] In a previous study, we employed the deuterium-labeled substrate probe **1** to analyze the stereochemical course of alkene amidopalladation with a number of different catalyst systems (Scheme 2A).[7a] Nearly all of the catalyst systems evaluated in this study showed exclusive preference for a *cis*-amidopalladation pathway. The only exception was (IMes)Pd(TFA)$_2$(OH$_2$). When this catalyst was employed in the absence of a basic additive, the reaction exhibited a

†Dedicated to the memory of Prof. Howard E. Zimmerman (July 5, 1926 – February 12, 2012), a revered colleague and pioneer in the field of physical organic chemistry, including organic photochemistry, applications of molecular orbital theory to organic chemical reactivity, and stereochemical implications of kinetically-controlled protonation steps.[1]

Correspondence to: Shannon S. Stahl, stahl@chem.wisc.edu.

Supporting Information Available: Experimental details, supplemental rate dependences and ^{1}H NMR spectra, and mathematical derivation of the rate law. This material is available free of charge via the Internet at http://pubs.acs.org.

mixture of products arising from both *cis*- and *trans*-amidopalladation pathways (*cis/trans* ~ 2:1). Very recently, we used another deuterium-labeled substrate probe **2** to examine the amidopalladation pathway with a $Pd(TFA)_2$ catalyst bearing a chiral pyridine-oxazoline ligand **3** (Scheme 2B).[7d] In this case, *trans*-amidopalladation is highly favored (*cis/trans* ~ 1:9).

The $(IMes)Pd(TFA)_2(H_2O)$-catalyzed oxidative heterocyclization reaction provides a unique opportunity to investigate the factors that influence the stereochemical course of the amidopalladation reaction. The balance between *cis*- and *trans*-amidopalladation observed in the absence of additives contrasts exclusive *cis*-amidopalladation when the reaction is carried out in the presence of Na_2CO_3 (Scheme 2A, entries 5 and 6). In order to understand the basis for this switch in selectivity, we have carried out systematic mechanistic investigations of $(IMes)Pd(TFA)_2(H_2O)$-catalyzed aerobic oxidative intramolecular amidation of (*Z*)-4-hexenyltosylamide under both conditions. Kinetic and isotope-labeling studies of these reactions reveal a number of key differences between the two reaction conditions, and the results highlight the kinetic influence of proton-transfer from the nitrogen nucleophile on the catalytic rate and the stereochemical course of alkene amidopalladation. Comparison between these results and those obtained with a $Pd(OAc)_2$/pyridine catalyst system[10] are also presented below.

Results

Kinetic Studies

The intramolecular aerobic oxidative amidation of (*Z*)-4-hexenyltosylamide **4** catalyzed by $(IMes)Pd(TFA)_2(H_2O)$ (5 mol%) proceeds to complete conversion in the presence of 2 equiv. Na_2CO_3 within 12 h at 80 °C (eq 1). A computer-interfaced gas-uptake apparatus was utilized to acquire the kinetics of the catalytic reaction by monitoring the change in oxygen pressure within a sealed, temperature-controlled reaction vessel. The reaction time-course reveals a monotonic decrease in pressure (Figure 1), thereby permitting the kinetic data to be analyzed by initial-rates methods.

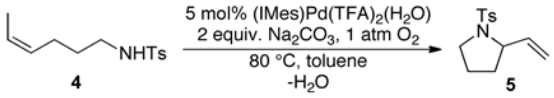

(1)

The initial kinetic study focused on the contribution of the primary reaction components (O_2, tosylamide, and catalyst) to the initial turnover rate. Data were acquired for reactions carried out in the presence and absence of exogenous base Na_2CO_3 (2 equiv). A zero-order rate dependence on the initial O_2 pressure was obtained, both in the presence and absence of added base, but the initial turnover rate of the oxidation reaction exhibits a nearly three-fold enhancement with added base (Figure 2). A saturation-like dependence on [**4**] was observed under both sets of conditions, and the initial oxidation rate plateaus at a lower [**4**] in the absence of exogenous base (Figure 3). Finally, a first-order dependence on $[(IMes)Pd(TFA)_2(H_2O)]$ is evident under conditions with and without added base (Figure 4).

The Hammett plot obtained with a series of *para*-substituted benzenesulfonamides (eq 2) reveals that there is negligible electronic effect on the catalytic turnover rate in the absence of exogenous base (Figure 5A). In contrast, the non-linear Hammett plot obtained in the presence of 2 equiv of exogenous base (Na_2CO_3) shows that benzenesulfonamides bearing

electron-withdrawing substituents react faster than the ones bearing electron-donating substituents (Figure 5B).

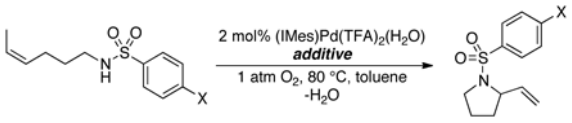

(2)

The dependence of initial turnover rates on the concentration of added trifluoroacetic acid was examined in the absence of exogenous base. A sharp inhibitory effect of [CF_3COOH] on the initial turnover rate was observed (Figure 6).

Kinetic Isotope Effects and Isotopic-labeling Studies

The dependence of the initial rate on [amide], measured with the CD_3-labeled tosylamide **4**-*d*$_3$, reveals a slight saturation dependence similar to that observed with the parent tosylamide **4** (eq 3, Figure 7). By comparing the initial rates from independent oxidative amidation reactions of tosylamides **4** and **4**-*d*$_3$ (Figure 7), a negligible kinetic isotope effect (k_{CH3}/k_{CD3} = 0.95) is evident.

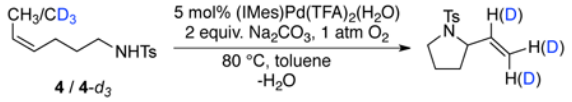

(3)

The mono-deuterium-labeled substrate **4**-*d*$_1$ was utilized to probe the intramolecular selectivity between β-hydride and β-deuteride elimination from the palladium-alkyl intermediate **6** (Scheme 3). Analysis of final products by ^{1}H NMR spectroscopy, however, revealed that deuterium is incorporated into the internal vinyl position, both in the presence and in the absence of exogenous base. These observations suggest that the β-hydride elimination step is reversible (see further discussion below). Experiments carried out with a 1:1 mixture of **4** and the CD_3-labeled tosylamide **4**-*d*$_3$ showed the formation of crossover products under both reaction conditions, arising from deuterium incorporation into the product originating from unlabeled **4** (Scheme 4). These observations show that deuterium exchange can take place in an *inter*molecular, as well as intramolecular, process. These deuterium exchange processes prevent determination of the intrinsic isotope effect for the β-hydride elimination step.

^{1}H NMR Spectroscopic Studies

^{1}H NMR spectroscopic studies were conducted to gain insights into the palladium speciation under catalytic conditions. Due to the lack of efficient liquid/solid mixing in the NMR tubes, only the homogeneous reaction conditions (without base) were investigated. Elevated pressures of oxygen gas (2–3 atm) were employed to ensure that adequate dissolved O_2 was present during the catalytic reaction. The ^{1}H NMR spectroscopic data suggested that (IMes)Pd(TFA)$_2$(L) (L = H_2O or tosylamide **4**) is the Pd resting state during catalytic turnover (conditions: 17 mol% (IMes)Pd(TFA)$_2$(H_2O), 0.0108 M tosylamide **4**, 80 °C, toluene-*d*$_8$). Evidence for coordination of tosylamide **4** to the catalyst

(IMes)Pd(TFA)$_2$(H$_2$O) was obtained by mixing the two components at room temperature in toluene-d_8. A plot of the ^{1}H NMR chemical shift of the NHC proton as a function of [**4**] is shown in Figure 8 (solid line).[11] To assess whether substrate coordination to Pd^{II} takes place via the alkene or the sulfonamide nitrogen lone pair, the same titration experiments were carried out with *N*-ethyltosylamide and cyclohexene under identical conditions (Figure 8, blue and green dotted lines, respectively). *N*-Ethyltosylamide induces a shift of the ^{1}H NMR resonances of the NHC ligand similar to that observed with tosylamide **4**, whereas no significant change in the NHC ligand resonances was observed upon addition of cyclohexene. These observations suggest that the initial interaction between **4** and the Pd^{II} center of the catalyst involves coordination of the sulfonamide nitrogen lone pair rather than the alkene. The addition of heterogeneous base Na$_2$CO$_3$ resulted in no observable change of either the ^{1}H or ^{19}F NMR spectra of (IMes)Pd(TFA)$_2$(H$_2$O) at temperatures ranging from −37 – 40 °C.

Discussion

Proposed Catalytic Mechanism

A general framework for the catalytic mechanism of (IMes)Pd(TFA)$_2$(H$_2$O)-catalyzed oxidative cyclization of **4** is depicted in Scheme 5, which includes both *cis*- and *trans*-amidopalladation pathways (*cis*-AP: **7** → **8** → **9**; *trans*-AP: **10** → **11** → **9**). The two amidopalladation pathways converge in the formation of Pd^{II}-alkyl intermediate **9**. Subsequent β-hydride elimination from **9** gives rise to the vinylpyrrolidine-coordinated Pd^{II}-hydride intermediate **12**. Product dissociation from the Pd^{II} center in **12** generates Pd^{II}-hydride intermediate **13**, which can undergo HX-reductive elimination. Aerobic oxidation of (IMes)Pd^0 regenerates the Pd^{II} catalyst.[12] The reversibility of the β-hydride elimination (**9** → **12**) and the vinylpyrrolidine dissociation (**12** → **13**) were demonstrated in the deuterium labeling study with substrate **4**-d_1 (Scheme 3) and the crossover experiment with tosylamides **4** and **4**-d_3 (Scheme 4), respectively.

Influence of Na$_2$CO$_3$ on the Catalytic Mechanism

In the presence of Na$_2$CO$_3$ as an added base, the cycle in Scheme 5 can be simplified by omitting the *trans*-amidopalladation pathway, which does not occur under these conditions.[7a] In this case, the oxidative amidation reaction is initiated by equilibrium formation of the Pd^{II}–amide adduct **7** (K_1^{cis}), followed by deprotonation of the sulfonamide nucleophile (k_2^{cis}). Insertion of the alkene into the palladium-amidate bond of **8** generates palladium-alkyl intermediate **9**.

The presence of heterogeneous Na$_2$CO$_3$ could promote this pathway and enhance the overall catalytic rate by facilitating deprotonation of the coordinated amide in **7**. The insolubilty of Na$_2$CO$_3$ in toluene complicates direct investigation of this step, but two possible roles of the carbonate base seem plausible. Preequilibrium proton transfer could take place within the coordination sphere of Pd^{II}, from the coordinated sulfonamide to the trifluoroacetate ligand, followed by dissociation of TFAH and irreversible deprotonation by the insoluble carbonate base. Alternatively, small amounts of CO_3^{2-} could exchange with TFA at the Pd^{II} center, and the more basic carbonate anion could facilitate deprotonation of the coordinated sulfonamide. These alternatives cannot be distinguished on the basis of the available data, but both processes could account for the enhanced catalytic rate and corresponding exclusive *cis*-amidopalladation of the alkene.

A rate law derived for this proposed mechanism (eq 4) rationalizes the saturation dependence on [**4**] and the first-order dependence on [(IMes)Pd(TFA)$_2$(H$_2$O)] (*cf.* Figures 3 and 4).[13] That the rate exhibits only a slight saturation dependence on [**4**] suggests that

sulfonamide coordination to Pd^{II} is not strongly favored, a conclusion consistent with the independent binding studies in Figure 8. Hammett data for the reaction with added Na_2CO_3 (*cf.* Figure 5B) indicate that sulfonamides with electron-withdrawing groups react more rapidly. This trend is expected if substrate deprotonation, **7** → **8**, is at least partially turnover limiting. The non-linearity of the Hammett plot may reflect a change in mechanism, but we speculate that these data arise from two (or more) steps contributing to the turnover rate (e.g., amide coordination and *N*–*H* deprotonation), each of which exhibits a different electronic dependence. Finally, the proposed mechanism accounts for the negligible kinetic isotope effect obtained from the reactions of tosylamides **4** and **4**-d_3 (*cf.* Figure 7), because β-hydride elimination step occurs after the turnover-limiting step.

$$\frac{d[\mathbf{5}]}{dt} = \frac{k_2^{cis} K_1^{cos} \bullet [\mathbf{4}] \bullet [\mathrm{Pd}]_T}{K_1^{cis} \bullet [\mathbf{4}] + [\mathrm{H_2O}]} \quad (4)$$

We recently reported a mechanistic study of the oxidative heterocylization of tosylamide **4** with $Pd(OAc)_2$/pyridine as the catalyst (eq 5).[10] Both $Pd(OAc)_2$/pyridine and (IMes)$Pd(TFA)_2(H_2O)$/Na_2CO_3 promote exclusive *cis*-amidopalladation of alkene; however, the reactions exhibit significantly different substrate electronic effects. Hammett analysis of $Pd(OAc)_2$/pyridine-catalyzed oxidative cyclization of **4** revealed a *negative* slope ($\rho = -0.22$) (Figure 9). This observation, together with additional kinetic and mechanistic data, are consistent with alkene insertion into a Pd–N bond as the turnover-limiting step in the $Pd(OAc)_2$/pyridine-catalyzed reaction. Briefly summarized, electron-withdrawing substituents enhance the acidity and increase the rate of deprotonation of the sulfonamide ligand with the (IMes)$Pd(TFA)_2(H_2O)$/Na_2CO_3 catalyst, whereas they decrease the nucleophilicity of the sulfonamidate and lower the rate of the nucleophilic attack on the alkene with the $Pd(OAc)_2$/pyridine catalyst. The different turnover-limiting steps with these two catalyst systems can be rationalized by the different relative basicities of the anionic ligands, trifluoroacetate vs. acetate. Specifically, the more basic acetate anion in the $Pd(OAc)_2$/pyridine catalyst results in sufficiently facile (and/or favorable) deprotonation of the amide that alkene insertion into the Pd–N bond becomes the turnover-limiting step.

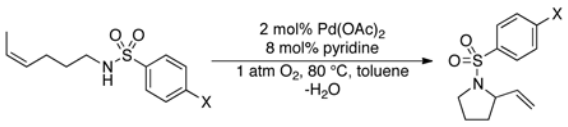

(5)

In the absence of base, the (IMes)$Pd(TFA)_2(H_2O)$-catalyzed intramolecular oxidative amidation of alkenes proceeds via both *cis*- and *trans*-amidopalladation pathways. Kinetic studies suggest the reaction exhibits a similar overall rate law under these conditions (*cf.* Figures 2–4), but it has a three-fold slower rate. Another noteworthy feature is the lack of a sulfonamide electronic effect on the rate (see Hammett plot in Figure 5B), which differs from the trends observed under the other two reaction conditions (*cf.* Figures 5A and 9). The result can be rationalized if the *cis*- and *trans*-amidopalladation pathways have offsetting electronic effects. Specifically, it is reasonable to expect that the *trans*-amidopalladation pathway has a negative Hammett slope associated with nucleophilic attack of a neutral sulfonamide on the coordinated alkene (i.e., more electron-rich nucleophiles react more rapidly; Scheme 5, **10** → **11**), while the *cis*-amidopalladation pathway exhibits a positive Hammett trend (Figure 5A). Since the rates of the *cis*- and *trans*-amidopalladation pathways

are finely balanced, variation of the *para*-substituent of benzenesulfonamide could simply shift the relative preference of one pathway over the other without significantly altering the overall rate. In support of this hypothesis, (IMes)Pd(TFA)$_2$(H$_2$O)-catalyzed oxidative amidation of *p*-nitrobenzenesulfonyl-substituted amide yields only the *cis*-amidopalladation product even in the absence of exogenous base.[5a]

Conclusion

This mechanistic study of (IMes)Pd(TFA)$_2$(H$_2$O)-catalyzed aerobic oxidative amidation of alkenes highlights the critical influence of "proton management" on the rate and stereochemical course of the catalytic reaction. Addition of an exogenous base (Na$_2$CO$_3$) enhances the turnover rate of the catalytic oxidative amidation reaction and shifts the mechanism to favor exclusively *cis*-amidopalladation of the alkene. These observations complement recent results obtained in a study of (pyrox)PdX$_2$-catalyzed enantioselective oxidative amidation of alkenes (*cf.* Scheme 2B).[7d] Use of the Pd(OAc)$_2$ catalyst (X = OAc) mediates *cis*-amidopalladation of the alkene, while the Pd catalyst with the less-basic trifluoroactate ligand (X = TFA) mediates *trans*-amidopalladation of the alkene. These results match those expected from the present study, which shows that basic conditions favor *cis*-amidopalladation. Collectively, these studies are beginning to provide the basis for rational development of Pd^{II} catalysts for oxidative heterofunctionalization of alkenes.

Experimental Section

General considerations

All commercially available compounds were purchased and used as received. Catalyst (IMes)Pd(TFA)$_2$(H$_2$O) was prepared as described previously. [15] (*Z*)-4-hexenyltosylamide **4**, *para*-substituted benzenesulfonamides, deuterium-labeled tosylamides **4**-*d*$_1$ and **4**-*d*$_3$ were all synthesized according to literature procedure.[10] ^{1}H NMR spectra were recorded on 300 and 500 MHz spectrometers. ^{1}H NMR chemical shifts (δ) are given in part per million relative to internal TMS (0.00 ppm). Ethylene glycol was used for temperature calibration of the NMR spectrometer for variable temperature measurements.

Representative procedure for gas-uptake kinetics

A typical reaction was conducted as follows: a 25 mL round-bottom flask with a stirbar was attached to an apparatus with a calibrated volume and a pressure transducer designed to measure the gas pressure within the sealed reaction vessel. The apparatus was evacuated to 10 torr and filled with oxygen to 800 torr and this cycle was repeated 10 times. The final pressure was established at 675 torr. After the pressure stablilzed within the apparatus, a stock solution of (IMes)Pd(TFA)$_2$(H$_2$O) (2.5 mM, in 3.6 mL toluene) was added via syringe through a septum. The flask was heated to 80 °C. After the temperature stabilized, a stock solution of tosylamide substrate (1.0 M, in 0.4 mL toluene) was added via syringe through a septum. Data was acquired using custom software written within LabVIEW. Correlations between oxygen uptake and conversions were made by ^{1}H NMR analysis with 1,3,5-trimethoxybenzene as an internal standard.

The procedure for the (IMes)Pd(TFA)$_2$(H$_2$O)-catalyzed oxidative amidation of **4** in the presence of Na$_2$CO$_3$ is similar to the above procedure, except that the 25 mL round-bottom flask was pre-charged with anhydrous Na$_2$CO$_3$ (*e.g.* 0.8 mmol).

Representative procedure for (IMes)Pd(TFA)$_2$(H$_2$O)-catalyzed aerobic oxidative cyclization of deuterium-labeled tosylamide 4-*d*$_1$

(IMes)Pd(TFA)$_2$(H$_2$O) (3 mg, 5 μmol) was placed in 13×100 mm disposable culture tubes. The reaction tubes were placed into a custom 48-well parallel reactor mounted on a large

capacity mixer and the headspace was purged with molecular oxygen for ca. 15 min. A solution of substrate probe **4**-d_1 (0.1 mmol) in toluene (1 mL) was added to tubes. The reactions were carried out for 24 h under an oxygen atmosphere (1 atm) at 80 °C. Following removal of the solvent under vacuum, the crude oxidative amination product was purified via column chromatography with hexanes/ethyl acetate and analyzed by ^{1}H NMR spectroscopy.

The procedure for the (IMes)Pd(TFA)$_2$(H$_2$O)-catalyzed oxidative amidation of **4**-d_1 in the presence of Na_2CO_3 is similar to the above procedure, except that the culture tube was pre-charged with both anhydrous Na_2CO_3 (0.2 mmol) and the catalyst.

Representative procedure for crossover experiments

(IMes)Pd(TFA)$_2$(H$_2$O) (3 mg, 5 μmol) was placed in 13×100 mm disposable culture tubes. The reaction tubes were placed into a custom 48-well parallel reactor mounted on a large capacity mixer and the headspace was purged with molecular oxygen for ca. 15 min. Solutions of a 1:1 mixture of tosylamides **4** and **4**-d_3 (0.1 mmol total) in toluene (1 mL) were added to tubes. The reactions were carried out for 24 h under an oxygen atmosphere (1 atm) at 80 °C. Following removal of the solvent under vacuum, the crude oxidative amination product was purified via column chromatography with hexanes/ethyl acetate. The purified product was dissolved in CH_2Cl_2 and submitted for mass spectroscopy measurement (ESI). The MS detector was set to avoid saturation in order to get accurate relative peak intensities in these experiments.

The procedure for the crossover experiment performed in the presence of Na_2CO_3 is similar to the above procedure, except that the culture tube was pre-charged with both anhydrous Na_2CO_3 (0.2 mmol) and the catalyst.

Catalytic reaction monitored by ^{1}H NMR spectroscopy

A freshly prepared solution of (IMes)Pd(TFA)$_2$(H$_2$O) and **4** (1.8 mM palladium, 10.8 mM **4**, 6.0 mM 1,3,5-trimethoxybenzene, in toluene-d$_8$, 0.7 mL) was added to a medium-wall NMR tube attached to a sealed 14/20 ground glass joint. The solution was frozen in liquid nitrogen. The NMR tube was connected to a gas manifold attached to a mercury monometer, both of which were calibrated for volume. The solution was degassed three times and then oxygen (0.263 mmol) was condensed in the tube to achieve a final pressure of 2.6 atm in the headspace above the solution. The solution was kept cold in a bath of dry ice/acetone until it was inserted into the spectrometer probe, preheated to 80 °C.

Supplementary Material

Refer to Web version on PubMed Central for supplementary material.

Acknowledgments

We are grateful to the NIH for financial support of this work (R01 GM67163).

References

1. (a) Schuster DI. Angew Chem Int Ed. 2012; 51:5286–5288.(b) Hixson SS, Mariano PS, Zimmerman HE. Chem Rev. 1973; 73:531–551.(c) Zimmerman HE. Acc Chem Res. 1987; 20:263–268.(d) Zimmerman HE, Nesterov EE. Acc Chem Res. 2002; 35:77–85. [PubMed: 11851385]
2. For reviews, see: Hegedus LS. Semmelhack MF. Comprehensive Organic Synthesis. Pergamon Press, IncElmsford1991; 4:551–569.Hosokawa T, Murahashi S-I. Negishi E, de Meijere A. Handbook of Organopalladium Chemistry for Organic Synthesis. John Wiley and Sons, IncNew

York2002; 2:2169–2192.Hosokawa T. Negishi E, de Meijere A. Handbook of Organopalladium Chemistry for Organic Synthesis. John Wiley and Sons, IncNew York2002; 2:2211–2225.Zeni G, Larock RC. Chem Rev. 2004; 104:2285–2309. [PubMed: 15137792] Stahl SS. Angew Chem, Int Ed. 2004; 43:3400–3420.Beccalli EM, Broggini G, Martinelli M, Sottocornola S. Chem Rev. 2007; 107:5318–5365. [PubMed: 17973536] Minatti A, Muñiz K. Chem Soc Rev. 2007; 36:1142–1152. [PubMed: 17576481] Kotov V, Scarborough CC, Stahl SS. Inorg Chem. 2007; 46:1910–1923. [PubMed: 17348722] McDonald RI, Liu G, Stahl SS. Chem Rev. 2011; 111:2981–3019. [PubMed: 21428440]

3. (a) Fix SR, Brice JL, Stahl SS. Angew Chem, Int Ed. 2002; 41:164–166.(b) Rogers MM, Wendlandt JE, Guzei IA, Stahl SS. Org Lett. 2006; 8:2257–2260. [PubMed: 16706500] (c) Scarborough CC, Bergant A, Sazama GT, Guzei IA, Spencer LC, Stahl SS. Tetrahedron. 2009; 65:5084–5092. [PubMed: 20161255] (d) McDonald RI, White PB, Weinstein AB, Tam CP, Stahl SS. Org Lett. 2011; 13:2830–2833. [PubMed: 21534607] (e) Lu Z, Stahl SS. Org Lett. 2012; 14:1234–1237. [PubMed: 22356620] (f) Redford JE, McDonald RI, Rigsby ML, Wiensch JD, Stahl SS. Org Lett. 2012; 14:1242–1245. [PubMed: 22352383]
4. (a) Larock RC, Hightower TR, Hasvold LA, Peterson KP. J Org Chem. 1996; 61:3584–3584. [PubMed: 11667199] (b) Trend RM, Ramtohul YK, Ferreira EM, Stoltz BM. Angew Chem, Int Ed. 2003; 42:2892–2895.(c) Yip KT, Yang M, Law KL, Zhu NY, Yang D. J Am Chem Soc. 2006; 128:3130–3131. [PubMed: 16522078] (d) He W, Yip KT, Zhu NY, Yang D. Org Lett. 2009; 11:5626–5628. [PubMed: 19905004] (e) Jiang F, Wu Z, Zhang W. Tetrahedron Lett. 2010; 51:5124–5126.(f) Jana R, Pathak TP, Jensen KH, Sigman MS. Org Lett. 2012; 14:4074–4077. [PubMed: 22873944]
5. Representative examples of cis-amidopalladation: Brice JL, Harang JE, Timokhin VI, Anastasi NR, Stahl SS. J Am Chem Soc. 2005; 127:2868–2869. [PubMed: 15740119] Liu G, Stahl SS. J Am Chem Soc. 2006; 128:7179–7181. [PubMed: 16734468] Isomura K, Okada N, Saruwatari M, Yamasaki H, Taniguchi H. Chem Lett. 1985:385–388.Ney JE, Wolfe JP. Angew Chem, Int Ed. 2004; 43:3605–3608.Ney JE, Wolfe JP. J Am Chem Soc. 2005; 127:8644–8651. [PubMed: 15954769] Nakhla JS, Kampf JW, Wolfe JP. J Am Chem Soc. 2006; 128:2893–2901. [PubMed: 16506768] Muñiz K, Hovelmann CH, Streuff J. J Am Chem Soc. 2007; 130:763–773. [PubMed: 18081279]
6. Representative examples of trans-amidopalladation: Åkermark B, Bäckvall JE, Siirala-Hansén K, Sjöberg K, Zetterberg K. Tetrahedron Lett. 1974; 15:1363–1366.Åkermark B, Bäckvall JE, Hegedus LS, Zetterberg K, Siirala-Hansén K, Sjöberg K. J Organomet Chem. 1974; 72:127–138.Hegedus LS, Allen GF, Waterman EL. J Am Chem Soc. 1976; 98:2674–2676.Bäckvall JE. Acc Chem Res. 1983; 16:335–342.Bäckvall JE, Björkman EE. Acta Chem Scand B. 1984; 38:91–93.Watson MP, Overman LE, Bergman RG. J Am Chem Soc. 2007; 129:5031. [PubMed: 17402733] Cochran BM, Michael FE. J Am Chem Soc. 2008; 130:2786–2792. [PubMed: 18254623] Sibbald PA, Rosewall CF, Swartz RD, Michael FE. J Am Chem Soc. 2009; 131:15945–15951. [PubMed: 19824646]
7. For studies employing stereospecifically deuterated substrates, see: Liu GS, Stahl SS. J Am Chem Soc. 2007; 129:6328–6335. [PubMed: 17439217] Bertrand MB, Neukom JD, Wolfe JP. J Org Chem. 2008; 73:8851–8860. [PubMed: 18942792] Mai DN, Wolfe JP. J Am Chem Soc. 2010; 132:12157–12159. [PubMed: 20718417] Weinstein AB, Stahl SS. Angew Chem, Int Ed. 2012; 51:11505–11509.
8. For studies of stoichiometric alkene insertion into Pd-N bonds of well-defined Pd-anilide or -amidate complexes, see: Hanley PS, Markovic D, Hartwig JF. J Am Chem Soc. 2010; 132:6302–6303. [PubMed: 20408534] Neukom JD, Perch NS, Wolfe JP. J Am Chem Soc. 2011; 132:6276–6277. [PubMed: 20397666] Hanley PS, Hartwig JF. J Am Chem Soc. 2011; 133:15661–15673. [PubMed: 21815675] Neukom JD, Perch NS, Wolfe JP. Organometallics. 2011; 30:1269–1277.White PB, Stahl SS. J Am Chem Soc. 2011; 133:18594–18597. [PubMed: 22007610]
9. For trapping of the amidopalladation intermediate with an exogenous ligand, see: Sibbald PA, Rosewall CF, Swartz RD, Michael FE. J Am Chem Soc. 2009; 131:15945–15951. [PubMed: 19824646]
10. Ye X, Liu G, Popp BV, Stahl SS. J Org Chem. 2011; 76:1031–1044. [PubMed: 21250706]
11. See Supporting Information for the corresponding NMR spectra.

12. For mechanistic studies of the reaction of O_2 with IMes-ligated Pd^{II}-hydride complexes, see Konnick MM, Guzei IA, Stahl SS. J Am Chem Soc. 2004; 126:10212–10213. [PubMed: 15315411] Konnick MM, Gandhi BA, Guzei IA, Stahl SS. Angew Chem, Int Ed. 2006; 45:2904–2907.Popp BV, Stahl SS. J Am Chem Soc. 2007; 129:4410–4422. [PubMed: 17371024] Konnick MM, Stahl SS. J Am Chem Soc. 2008; 130:5753–5762. [PubMed: 18393426] Konnick MM, Decharin N, Popp BV, Stahl SS. Chem Sci. 2011; 2:326–330.
13. See Supporting Information for the mathematical derivation of rate laws.
14. Note: The original Hammett plot reported in ref. 10 featured incorrect *y*-axis labels; however, the reported ρ value (−0.22) is correct. The corrected axes are included in Figure 9.
15. Sigman and coworkers reported the use of $(IMes)Pd(TFA)_2(H_2O)$ and related complexes as catalysts for aerobic alcohol oxidation. See: Jensen DR, Schultz MJ, Mueller JA, Sigman MS. Angew Chem, Int Ed. 2003; 42:3810–3813.Mueller JA, Goller CP, Sigman MS. J Am Chem Soc. 2004; 126:9724–9734. [PubMed: 15291576]

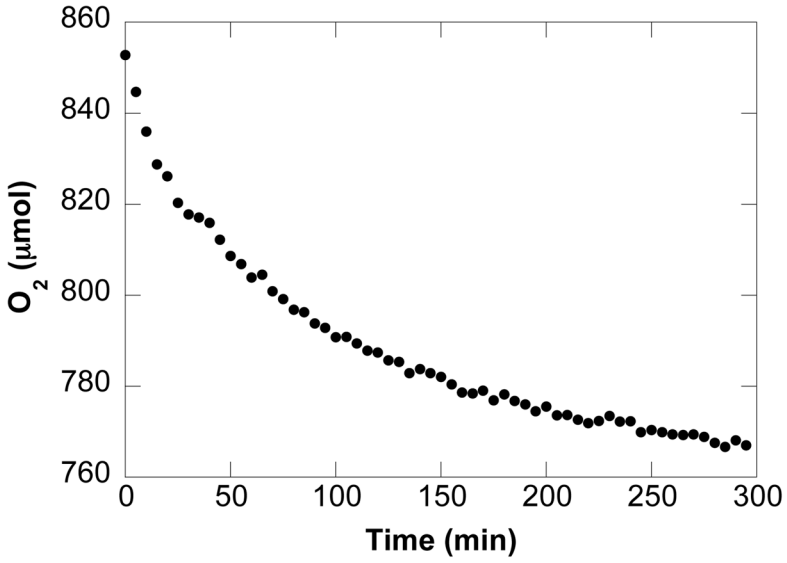

Figure 1.

A representative kinetic time course for (IMes)Pd(TFA)$_2$(H$_2$O)-catalyzed intramolecular oxidative amidation of (*Z*)-4-hexenyltosylamide **4** obtained by gas-uptake methods. Data sampling occurred at a rate of 1 s^{-1} (not all data are shown). Conditions: [(IMes)Pd(TFA)$_2$(H$_2$O)] = 2.0 mM, [**4**] = 0.10 M, 0.8 mmol Na_2CO_3, 4.0 ml of toluene, initial pO_2 = 700 torr, 4.0 ml of toluene, 80 °C.

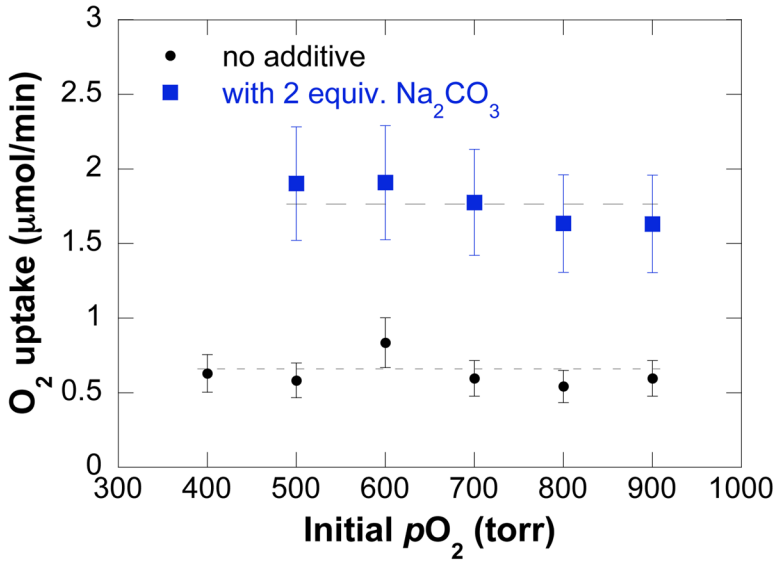

Figure 2.

Dependences of the initial rate on the initial oxygen pressure in the presence and absence of 2 equiv. of exogenous base Na_2CO_3. Conditions: [(IMes)Pd(TFA)$_2$(H_2O)] = 2.0 mM, [**4**] = 0.1 M, 4.0 ml of toluene, initial pO_2 = 400 – 900 torr, 80 °C. In the measurement of pO_2 dependence in the presence of base, 0.8 mmol Na_2CO_3 was used.

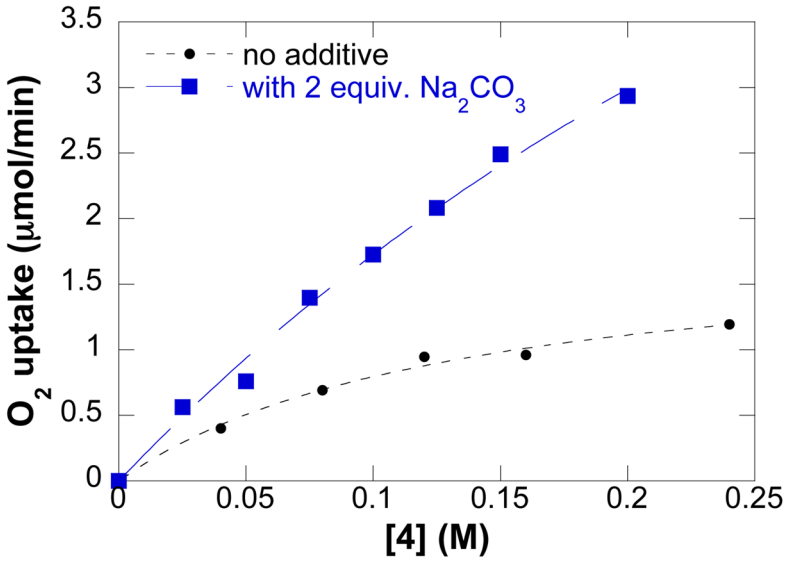

Figure 3.

Dependences of the initial rate on amide concentration in the presence and absence of 2 equiv. of exogenous base Na_2CO_3. The curve fit results from a nonlinear least-squares fit to a hyperbolic function of [**4**]. Conditions: [(IMes)Pd(TFA)$_2$(H_2O)] = 2 mM, [**4**] = 0 – 0.24 M, 4.0 ml of toluene, initial pO_2 = 700 torr, 80 °C. In the experiments with added base, 0.2 – 1.6 mmol Na_2CO_3 was used.

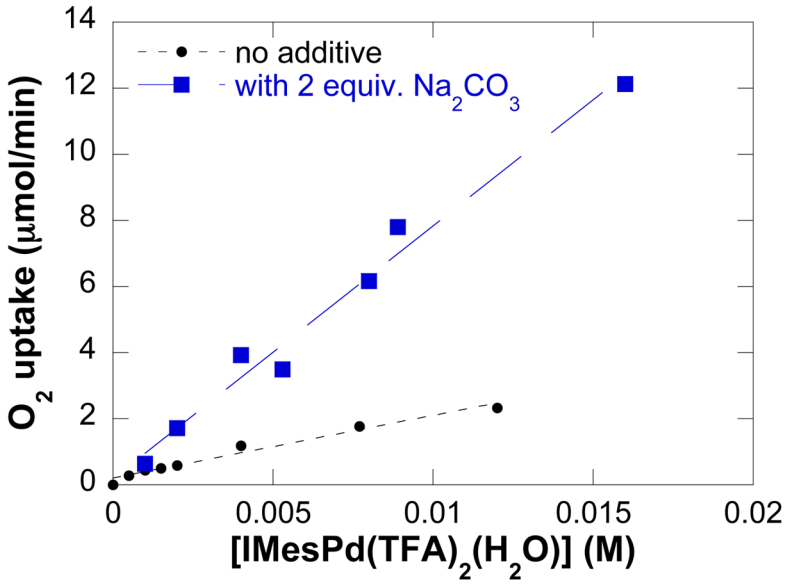

Figure 4.

Dependences of the initial rate on catalyst concentration in the presence and absence of 2 equiv. of exogenous base Na_2CO_3. The curve fit results from a fit to a linear function of [IMesPd(TFA)$_2$(H$_2$O)]. Conditions: [(IMes)Pd(TFA)$_2$(H$_2$O)] = 0 – 16 mM, [**4**] = 0.1 M, 4.0 ml of toluene, initial pO_2 = 700 torr, 80 °C. In the experiments with added base, 0.8 mmol Na_2CO_3 was used.

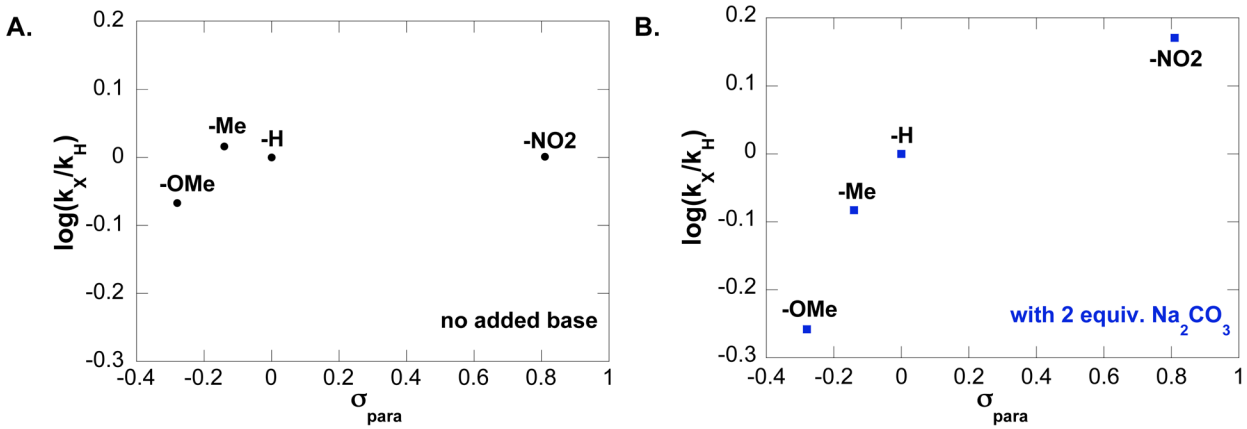

Figure 5.

Hammett plots obtained from the relative initial rates of catalytic oxidative amidation conducted with a series of *para*-substituted benzenesulfonamides. (A) Hammett plot in the absence of exogenous base. Conditions: [(IMes)Pd(TFA)$_2$(H$_2$O)] = 2 mM, [benzenesulfonamide] = 0.1 M, 4.0 ml of toluene, initial pO$_2$ = 700 torr, 80 °C. (B) Hammett plot in the presence of 2 equiv. exogenous base Na$_2$CO$_3$. Conditions: [(IMes)Pd(TFA)$_2$(H$_2$O)] = 2 mM, [benzenesulfonamide] = 0.1 M, 4.0 ml of toluene, initial pO$_2$ = 700 torr, 0.8 mmol Na$_2$CO$_3$, 80 °C.

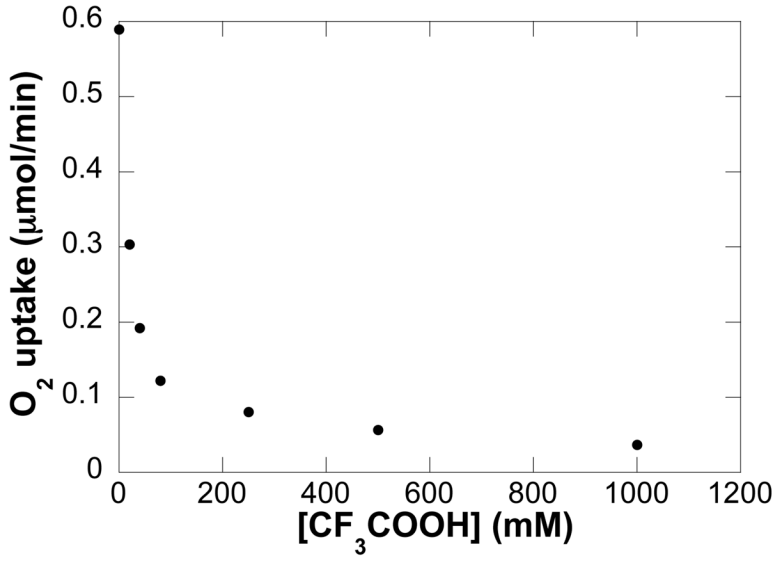

Figure 6.

Dependence of the initial rate on added CF_3COOH concentration in the absence of added base. Conditions: [(IMes)Pd(TFA)$_2$(H_2O)] = 2 mM, [**4**] = 0.1 M, [CF_3COOH] = 0 – 1 M, 4.0 ml of toluene, initial pO_2 = 700 torr, 80 °C.

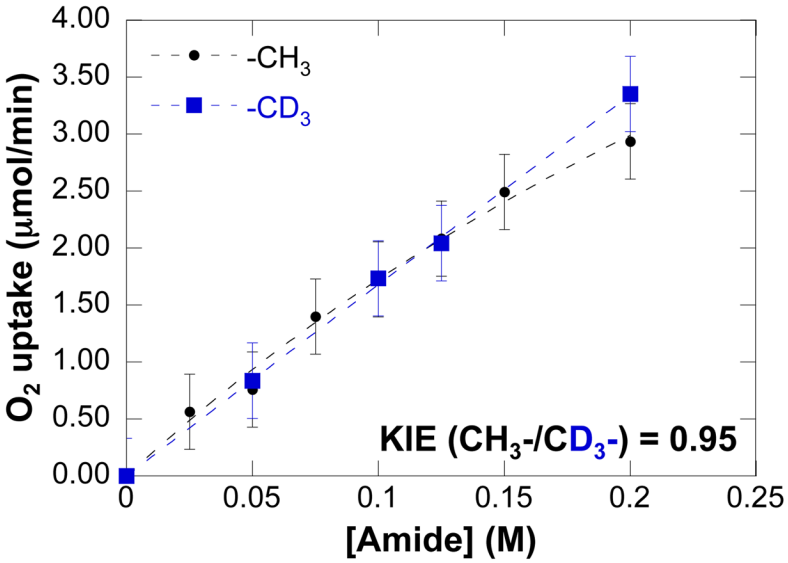

Figure 7.

Dependences of the initial O_2 uptake rate on [amide] (amide = **4** or **4**-*d*$_3$). Conditions: [(IMes)Pd(TFA)$_2$(H_2O)] = 2 mM, [amide] = 0 – 200 mM, 2 equiv. Na_2CO_3 relative to amide, 4.0 ml of toluene, initial pO_2 = 700 torr, 80 °C.

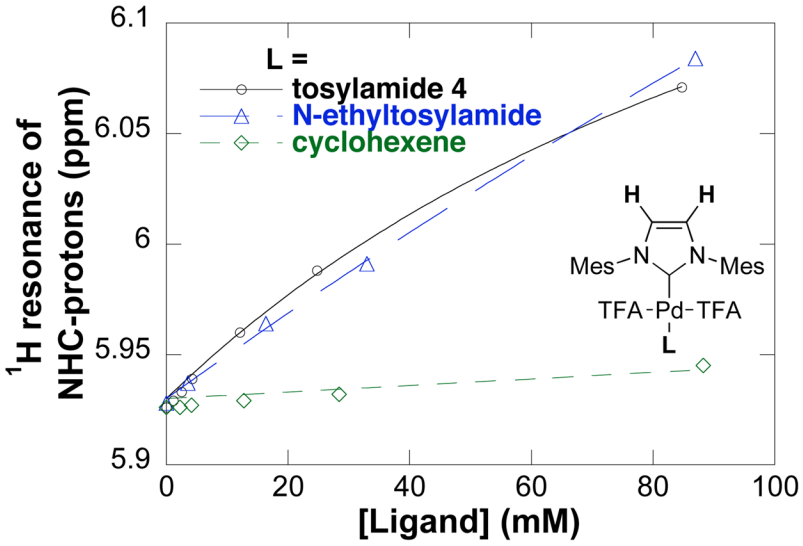

Figure 8.

Dependence of ^{1}H NMR chemical shift of the backbone protons of the IMes ligand in (IMes)Pd(TFA)$_2$(L) (L= H_2O, **4**, *N*-ethyltosylamide, or cyclohexene) on ligand concentration in the absence of added base Na_2CO_3. The curve fit results from a nonlinear least-squares fit to a hyperbolic function of [ligand]. Conditions: [(IMes)Pd(TFA)$_2$(H_2O)] = 5 mM, [Ligand] = 0 – 0.08 M, in toluene-d_8, 24 °C.

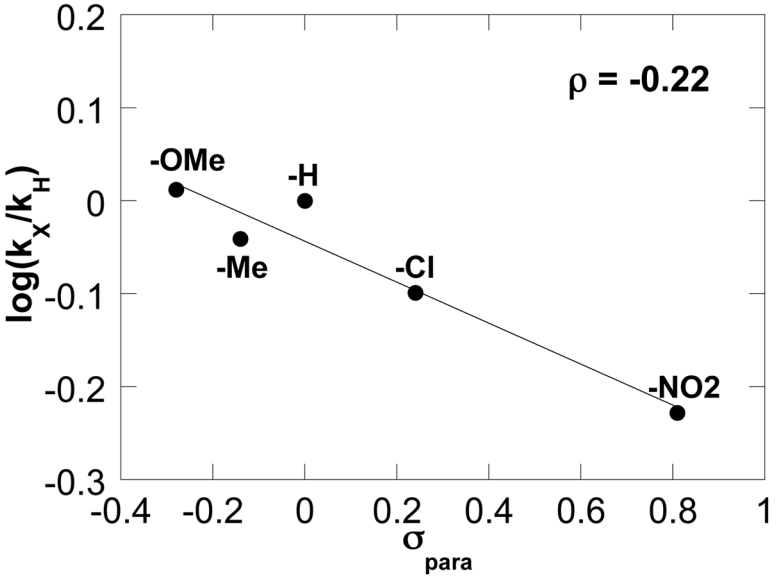

Figure 9.

Hammett correlation of the $Pd(OAc)_2$/pyridine-catalyzed oxidative heterocyclization (data replotted from ref. 10[14]). Conditions: [$Pd(OAc)_2$] = 2.0 mM, [pyridine] = 8.0 mM, [amide] = 100 mM, 4.0 ml of toluene, initial pO_2 = 700 torr, 80 °C.

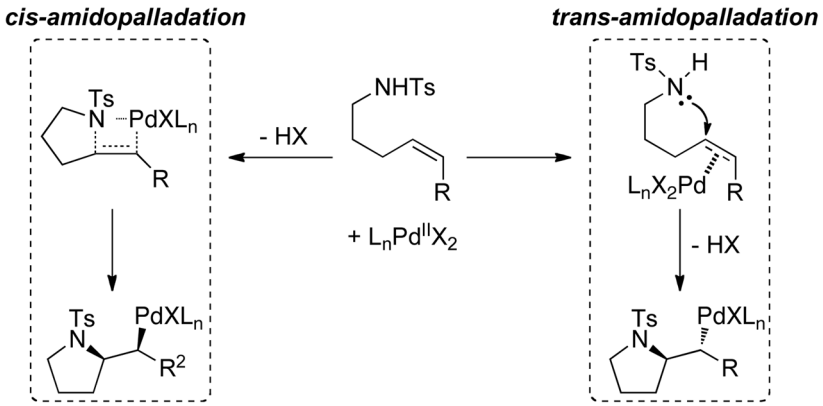

Scheme 1.
Cis- vs. *Trans*-Amidopalladation of Alkenes.

A.

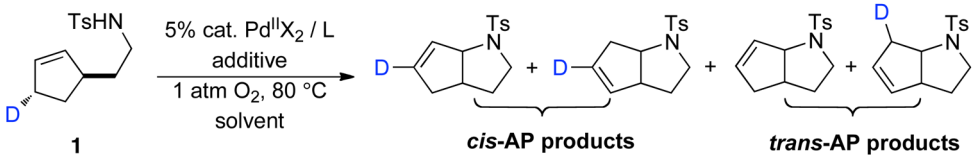

Entry	Catalyst System	Solvent	Additive	*cis*-AP : *trans*-AP
1	$Pd(OAc)_2$	DMSO	—	100 : 0
2	$Pd(OAc)_2$ / pyridine	toluene	—	100 : 0
3	$Pd(TFA)_2$ / pyridine	toluene	2 eq Na_2CO_3, 3Å M.S.	100 : 0
4	$Pd(TFA)_2$ / (–)-sparteine	toluene	2 eq N(*i*-Pr)$_2$Et, 3Å M.S.	100 : 0
5	(IMes)Pd(TFA)$_2$(H_2O)	toluene	—	**66 : 34**
6	(IMes)Pd(TFA)$_2$(H_2O)	toluene	2 eq Na_2CO_3	**100 : 0**

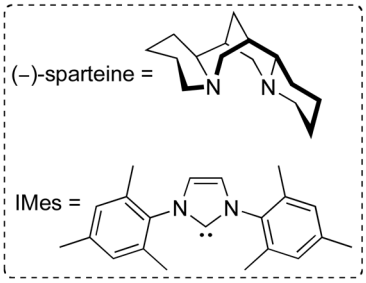

B.

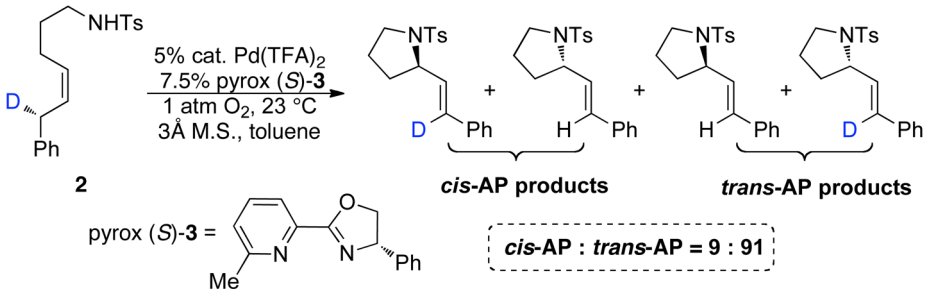

Scheme 2.

Stereochemical Probe Experiments for the Pd-Catalyzed Oxidative Amidocyclizations.[7a,d]

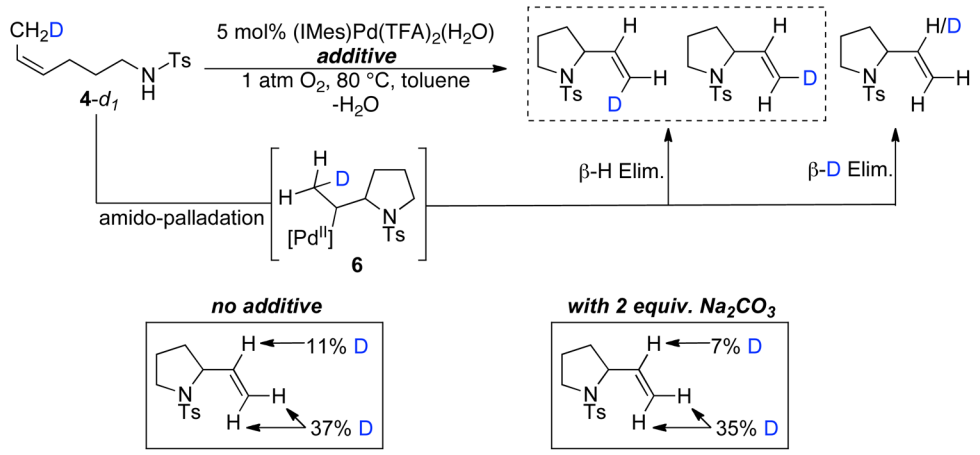

Scheme 3.

Isotopic-Labeling Studies with Substrate Probe **4**-d_1 and Evidence for Deuterium Exchange.

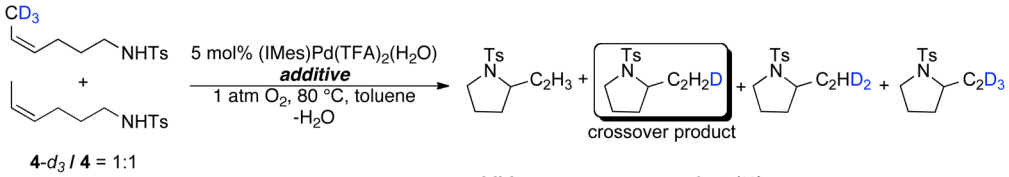

additive	crossover product (%)
none	23%
2 equiv. Na_2CO_3	16%

Scheme 4.

Crossover Experiments with 1:1 Mixture of Tosylamides **4**-d_3 and **4**, Providing Evidence for Intermolecular H/D Exchange.

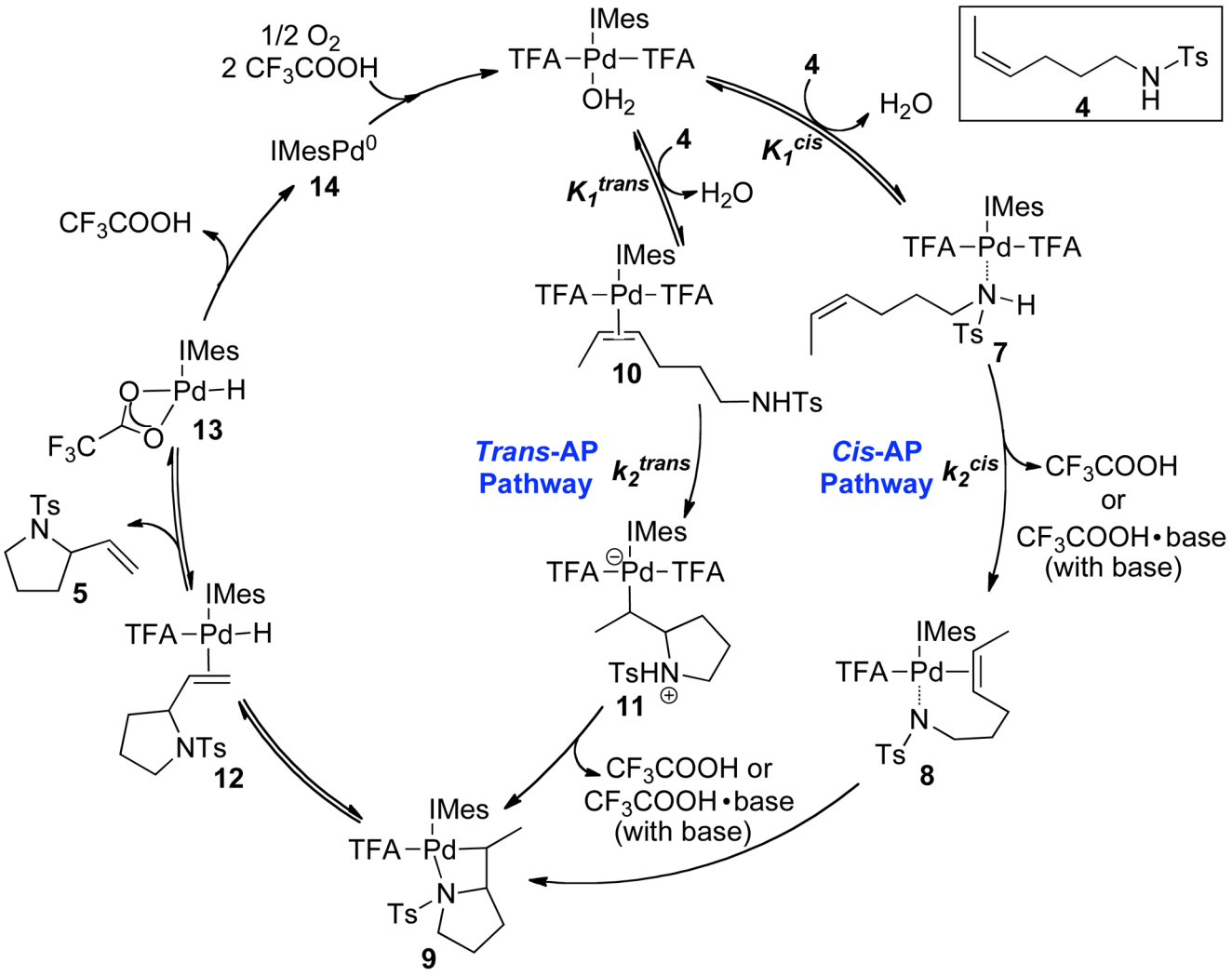

Scheme 5.

Proposed General Catalytic Mechanism for the (IMes)Pd(TFA)$_2$(H$_2$O)-Catalyzed Oxidative Amidocyclization of **4**.